Polarization optical nonlinearities in colloidal silver aggregates

V.P. Drachev,[1] S.V. Perminov,[1] S.G. Rautian,[2] V.P. Safonov,[2] and E.N. Khaliullin[1]

[1] Institute of Semiconductor Physics,
Siberian Branch of the Russian Academy of Sciences, Novosibirsk
[2] Institute of Automation and Electrometry,
Siberian Branch of the Russian Academy of Sciences, Novosibirsk

Received April 11, 2001

We study the local and nonlocal optical responses from a cubic-nonlinear isotropic medium – aggregated colloidal silver solution. Nonlinear polarization effects in the pump-probe technique are considered phenomenologically. The inverse Faraday effect, optical Kerr effect, and self-induced rotation of the polarization ellipse in a disordered fractal medium were observed for the first time. The components of the tensors of local and nonlocal nonlinearities of colloidal silver solutions with different degree of aggregation were measured.

Introduction

Many processes occurring under natural conditions and in laboratory experiments involve aggregation of solid particles wandering in a gas or liquid that may form clusters having an irregular branched structure. Large clusters produced, in particular, at aggregation in colloidal solutions consist of hundreds and thousands of nanoparticles and have a fractal structure.[1] Optical properties of random clusters differ from the properties of both the continuum and of isolated small particles (monomers) constituting clusters.

Thus, aggregation of noble metal particles into clusters leads to a giant enhancement of Raman scattering on molecules adsorbed on metal particles.[2] In Ref. 3, it was predicted that nonlinear optical responses from aggregates increase markedly as compared to isolated nanoparticles. In the experiments with silver nanocomposites, giant enhancement of degenerated four-photon scattering[4] and second harmonic generation[5] were observed at aggregation of silver particles into clusters. Then, the processes of nonlinear refraction and nonlinear absorption[6,7] and third harmonic generation[8] in aggregated colloidal solutions of noble metals were studied. Nonlinear optical effects in clusters may prove to be important for particles of natural media as well. This is especially true for the effect of coupled enhancement of optical responses from clusters inside a microcavity,[9] because the microscopic droplets with high Q-factor for the optical modes constitute an important component of aerosol.[10]

In theoretical analysis of the optical properties of fractal clusters, the model of coupled dipoles is widely used.[3,11,12] According to this model, the light field induces oscillating dipole moments on highly polarized metal particles. The interaction of the light-induced dipole moments leads to formation of collective modes of dipole excitation in clusters. Just these modes determine optical properties of the nanocomposites.

The eigenfrequencies of the collective modes cover a wide (up to 10^4 cm^{-1}) spectral region. The spatial configurations of the collective modes characterized by the electric field distribution widely vary. In particular, optical excitation may concentrate in a small zone as compared to the aggregate size and the wavelength.[13,14] Such concentration leads to a significant enhancement of the local electric field. This circumstance is especially important for the nonlinear optical processes depending on the square, cubic, and higher-order electric field. We can state that now there is a qualitative agreement between the theoretical conclusions[12] and the experimental results obtained when studying the spectra of linear absorption,[15] selective photomodification,[14] four-wave interaction,[4] and harmonics generation[5] in silver aggregates.

Polarization optical nonlinearities of metal nanocomposites are less thoroughly studied. At the same time, polarization effects bear important information on the substance studied. Polarization phenomena are widely used in the development of laser radiation control methods and optical recording of information. In Ref. 16, we described observations of nonlinear optical activity (NOA) of fractal silver aggregates due to spatial dispersion of the third-order nonlinear response (in other words, nonlinear character of medium interaction with the field of a light wave). However, it is well known that a wave in an isotropic medium may also change due to purely local cubic inhomogeneity. If the radiation polarization differs from the strictly linear or circular, then polarization self-action consisting in rotation of the polarization ellipse takes place.[17]

Nonlinear polarization effects occur also at two-wave interaction. The interaction of two waves [strong (pump) and probe ones] in a nonlinear medium with a local response changes polarization of the probe wave (except for the situation that both waves are linearly polarized in the same plane). Such effects include, in particular, the inverse Faraday effect (IFE), i.e.,

0235-6880/01/05 326-06 $02.00

rotation of the polarization plane of the probe field at circularly polarized pumping,[18] and the optical Kerr effect (OKE), i.e., induction of birefringence in the isotropic medium by a linearly polarized strong wave.[19]

In this paper we consider polarization nonlinearities of colloidal silver aggregates. Our measurements have demonstrated rather high values of IFE and OKE for silver nanoaggregates.

1. Polarization self-action and interaction of light waves in cubic-nonlinear medium

Cubic nonlinear polarization of a medium in the general case involves two terms:

$$\tilde{\mathbf{P}}^{(3)}(\mathbf{r}, t) = \hat{\chi}^{(3)}\mathbf{EEE} + \hat{\Gamma}^{(3)}\,\mathbf{EE}\nabla\mathbf{E}. \qquad (1)$$

The first term in the right-hand side of Eq. (1) is responsible for the local nonlinear third-order response from the medium, and the second term allows for the spatial dispersion of the nonlinear response.

In an isotropic medium, an intense monochromatic field $\mathbf{E}(\mathbf{r}, t) = \mathbf{A}\exp[i(\mathbf{kr} - \omega t)] + \text{c.c.}$ induces nonlinear polarization of the following form[20]:

$$\mathbf{P}^{(3)}(\omega) = \chi_1\mathbf{A}(\mathbf{AA}^*) + \chi_2\mathbf{A}^*(\mathbf{AA}) - ig_1\{(\mathbf{AA}^*)\mathbf{k}\times$$
$$\times\,\mathbf{A} + \mathbf{A}(\mathbf{A}^*[\mathbf{k}\times\mathbf{A}])\}, \qquad (2)$$

where $\chi_1 = 6\chi^{(3)}_{iijj} = 6\chi^{(3)}_{ijij}$; $\chi_2 = 3\chi^{(3)}_{ijji}$; $i, j = 1, 2$; g_1 is the single (ignoring the frequency dispersion) independent component of the tensor $\hat{\Gamma}^{(3)}$.

Substituting the polarization (2) into the wave equation, we can obtain the equation (similarly to that obtained in Ref. 20) for the slow amplitude of the wave propagating in the nonlinear medium

$$\frac{\mathrm{d}A_\pm}{\mathrm{d}z} = -\delta A_\pm + i\frac{2\pi\omega^2}{kc^2}\times$$
$$\times\{(\chi_1|A|^2 + 2\chi_2|A_\mathrm{K}|^2) \pm 2kg_1|A_\pm|^2\}A_\pm, \qquad (3)$$

where $\delta = (\omega^2/2kc^2)\,\mathrm{Im}\varepsilon^{(1)}$ is the amplitude coefficient of linear absorption; $\varepsilon^{(1)} = n_0^2$ is the linear medium permittivity; $A_\pm$ are circular components of the complex amplitude connected with the Cartesian components $A_{1,2}$: $A_\pm = (A_1 \pm iA_2)/\sqrt{2}$. We do not consider here the natural (linear with respect to the filed) optical activity, and the corresponding term is omitted in Eq. (3) and below.

From Eq. (3) we can derive the equation for the azimuth of the polarization ellipse $\alpha = \arg(A_+A_-^*)/2$ as the wave propagates in the medium:

$$\frac{\mathrm{d}\alpha}{\mathrm{d}z} = \frac{2\pi\omega}{n_0c}\,\mathrm{Re}\chi_2(|A_-|^2 - |A_+|^2) + \frac{2\pi\omega^2}{c^2}|A|^2\,\mathrm{Re}g_1. \qquad (4)$$

The first term in the right-hand side of the equation corresponds to the known effect of self-induced rotation of the polarization ellipse[17] in the isotropic medium with local cubic nonlinearity. The second term describes the nonlinear optical activity due to spatial dispersion of the nonlinear response.

Now let us pass to analysis of nonlinear polarization effects in the pump-probe technique. Having in mind the study of IFE and OKE, we assume the nonlinear response to be local. The electric field is considered as a sum of two quasiplane waves with the same frequencies, but different wave vectors:

$$\mathbf{E}(\mathbf{r},t) = [\mathbf{F}\exp(i\mathbf{Kr}) + \mathbf{S}\exp(i\mathbf{kr})]\exp(-i\omega t) + \text{c.c.}, \qquad (5)$$

where $\mathbf{F}$, $\mathbf{K}$ and $\mathbf{S}$, $\mathbf{k}$ are complex amplitudes and wave vectors of, respectively, the pump and the probe waves. The dependence of $\mathbf{F}$ and $\mathbf{S}$ on $\mathbf{r}$ is assumed slow as compared to the exponential factor.

Substitute Eq. (5) into Eq. (2) and, assuming the probe wave to be weak, consider only the terms linear with respect to $\mathbf{S}$. We obtain the following equation for the complex amplitude of the nonlinearly polarized wave with the wave vector $\mathbf{k}$:

$$\mathbf{P}^{(3)}_{\mathrm{loc}}(\mathbf{k},\omega)) = \chi_1[(\mathbf{F}^*\mathbf{F})\mathbf{S} + (\mathbf{F}^*\mathbf{S})\mathbf{F}] + 2\chi_2(\mathbf{FS})\mathbf{F}^*. \qquad (6)$$

Then, substitute the equation for the electric field in the form $\mathbf{E} = \mathbf{S}\exp[-i(\omega t - kz)] + \text{c.c.}$ and the equation for the nonlinear polarization in the form $\tilde{\mathbf{P}}^{(3)} = \mathbf{P}^{(3)}_{\mathrm{loc}}\exp[-i(\omega t - kz)] + \text{c.c.}$ into the wave equation. We derive the following equation for the complex amplitude of the probe field:

$$\frac{\mathrm{d}\mathbf{S}}{\mathrm{d}z} = -\delta\mathbf{S} + i\frac{2\pi\omega^2}{kc^2}\mathbf{P}^{(3)}_{\mathrm{loc}}. \qquad (7)$$

Let the basis vector $\mathbf{e}_z$ (hereinafter the Cartesian coordinates are denoted by subscripts x, y, and z) be directed along the vector $\mathbf{k}$. The angle between the wave vectors $\mathbf{K}$ and $\mathbf{k}$ is assumed small enough so that we can neglect the components F_z and K_x, K_y. Let us consider the relations between the polarizations of the pump and the probe fields in a more detail.

Inverse Faraday effect. Let the strong wave be circular polarized (clockwise, for definiteness), $F_- = 0$ and the probe wave be linearly polarized. We are interested in rotation of the polarization plane of the probe wave. This nonlinear effect is known in the literature as the inverse Faraday effect.

Rewriting Eq. (7) in circular coordinates, we have:

$$\frac{\mathrm{d}}{\mathrm{d}z}\begin{pmatrix}S_+\\S_-\end{pmatrix} = -\delta\begin{pmatrix}S_+\\S_-\end{pmatrix} + i\frac{2\pi\omega^2}{k_3c^2}|F_+|^2\begin{pmatrix}2\chi_1 & 0\\0 & \chi_1\end{pmatrix}\begin{pmatrix}S_+\\S_-\end{pmatrix}, \qquad (8)$$

wherefrom we derive the following equation for the angle of rotation of the polarization plane:

$$\frac{\mathrm{d}\alpha}{\mathrm{d}z} = \frac{\pi\omega}{cn_0}|F_+|^2\,\mathrm{Re}(\chi_1 - 2\chi_2). \qquad (9)$$

Optical Kerr effect. Consider now the other case. Let both waves have linear polarization and the strong wave be polarized along the axis x: $F_y = 0$; the direction of polarization of the probe wave makes a 45°

angle with that of the strong wave, so that $S_x = S_y$. As known, the linearly polarized strong field induces anisotropy of the refractive index in the medium, i.e., the medium becomes birefringent. As a result, a phase shift arises between the components S_1 and S_2 of the probe field, and this leads to the change in the elliptic polarization.

To find the value of the induced birefringence, let us write Eq. (7) in the Cartesian coordinates:

$$\frac{\mathrm{d}}{\mathrm{d}z}\begin{pmatrix}S_1\\S_2\end{pmatrix} = -\delta\begin{pmatrix}S_1\\S_2\end{pmatrix} + \\ + i\frac{2\pi\omega^2}{c^2k_3}|F_1|^2\begin{pmatrix}2(\chi_1+\chi_2) & 0\\ 0 & \chi_1\end{pmatrix}\begin{pmatrix}S_1\\S_2\end{pmatrix}. \qquad (10)$$

The nonlinear phase shift between the x- and y-components is determined by the equation $\Delta\varphi^{\mathrm{nl}} = \arg(S_1S_2^*)$ and satisfies the following equation:

$$\frac{\mathrm{d}\Delta\varphi^{\mathrm{nl}}}{\mathrm{d}z} = \frac{2\pi\omega}{cn_0}|F_1|^2\,\mathrm{Re}(\chi_1+2\chi_2). \qquad (11)$$

2. Measurement technique and experimental results

We studied the ethanol colloidal solution of silver. The solution was prepared by reduction of silver from $AgNO_3$ in the solution containing NaOH and polyvinylpyrrolidone with the mean molecular weight of 360 000. This technique is described in Ref. 21, and such a colloid is denoted hereinafter as Ag(PVP). According to the electron-microscopy data, the typical diameter of nanoparticles in the colloidal solution prepared in such a way is ~10 nm.

Two colloid samples with different degree of aggregation were studied. Nanoparticles in the colloid 1 form clusters consisting of hundreds of monomers. Analysis of microphotos shows that the clusters have a fractal structure with the size of a fractal $D \approx 1.8$. The solution 2 is weak-aggregated; it contains clusters consisting of several particles. The spectra of linear absorption (i.e., absorption in a weak field) of these samples are given in Ref. 16. The absorption spectrum of the weak-aggregated colloid 2 has a peak in the region of 400 nm due to excitation of a surface plasmon in isolated nanoparticles and a low "wing" in the visible region. The higher-aggregated colloid 1 is characterized by higher absorption in the long-wave wing due to excitation of collective plasmon modes in the clusters. For experiments, both of the colloids were diluted with ethanol in the same proportion (roughly 1:5) for the transmittance of the colloid 1 at the wavelength of 532 nm to be about 50%.

We used the second harmonic of a pulsed Nd:YAG laser with the pulse duration $\tau \sim 10$ ns and the wavelength of 532 nm. After a frequency doubler, the radiation passed through a polarizer (Glan prism), which provided us to reduce the residual elliptic polarization down to ~10^{-5} level in intensity. Then the radiation was split into two beams: the pump one and the probe, which were focused into a 3-mm-thick cell from fused silica containing the silver solution under study. The caustic waist diameter (at the level of $1/e$) was 0.5–0.6 mm for both beams, and the pump/probe power ratio was roughly 13. Signals were recorded with photodiodes with the time constant of 10 μs.

In the experiments with the probe field (IFE, OKE), we measured the parameters of the probe beam having passed through the polarimeter. In the experiments on studying self-action effects (NOA, self-induced rotation of the polarization ellipse), the probe beam was cut off, and the parameters of the strong field were measured.

In processing the obtained results, we took into account that in the actual experiment the intensity of the pump field always has some distribution in space and time. In our measurements, slow photodetectors were used, and we actually measured time-averaged values. The dimension of the photodiode sensitive area exceeded the diameter of the beams; therefore, we recorded signals averaged over the beam cross section. Assuming the intensity distribution in time and in the cross section to be Gaussian, we can readily find that allowance for averaging over space and time gives the factor $2\sqrt{2}$.

Self-action effects. When developing the measurement technique, we took into account the following circumstances. In a medium non-gyrotropic in the linear approximation, nonlinear rotation of the polarization plane of a linearly polarized wave ($|A_+|^2 = |A_-|^2$) is caused only by the nonlocal character of the nonlinear response. In Eq. (4), the term including g_1 corresponds to this effect. In the case of the elliptic polarization, additional rotation of the polarization plane connected with the local nonlinear response (term with $\mathrm{Re}\chi_2$) occurs. Since under experimental conditions the radiation polarization is always slightly elliptic, both of these terms should be taken into account. To separate the contributions of the local and nonlocal responses, the method we proposed in Ref. 16 was applied. The idea of this method is as follows. Note that in Eq. (4) $|A_+|^2 - |A_-|^2 = 2|A_x||A_y|\sin(\phi_x - \phi_y)$, where $|A_{x,y}|$ and $\phi_{x,y}$ are the amplitudes and phases of the linearly polarized field components. Varying the phase difference $\phi_x - \phi_y$, we can change the contribution of the local response with the contribution of the nonlocal response unchanged.

The experimental setup and the measurement technique were described in detail in Ref. 16. Measurements of the *nonlinear rotation of the polarization plane* gave the following results. The effect of nonlinear optical activity strongly depends on the degree of aggregation. The value of $\alpha_g/I_{\mathrm{eff}} \propto \mathrm{Re}\Gamma^{(3)}$ for the colloid 1 turned out to be roughly 80 times higher than that for the colloid 2: $\mathrm{Re}\Gamma_1^{(3)} \approx 0.9 \cdot 10^{-16}$ CGSE, $\mathrm{Re}\Gamma_2^{(3)} \approx 1.1 \cdot 10^{-18}$ CGSE. In both cases, the medium turned out to be counterclockwise rotating. The causes

for appearance of NOA and the sign of rotation can hardly be explained now.

To find the constant χ_2, we conducted the experiment on measuring the angle of rotation of the polarization ellipse of a strong field when passed through a nonlinear medium. The measurements were conducted using the colloidal solution 1. As the radiation intensity at the entrance to the cell changed from 0.7 to 5 MW/cm^2, the polarization ellipse has turned by $\alpha_{SR} \approx -(1.8 \pm 0.2)$ mrad for the clockwise polarization and $\alpha_{SR} \approx (2.1 \pm 0.2)$ mrad for the counterclockwise polarization at the eccentricity $|F_y|^2/|F_x|^2 \approx 1{:}6$. As is seen, the rotation angles have slightly different absolute values for both of the circular polarizations. This may be a manifestation of the nonlinear gyrotropy, according to Eq. (4) and roughly corresponds to NOA at 5 MW/cm^2. Taking a half-difference of these values, we can exclude the effect of NOA and calculate the value of χ_2:

$$\mathrm{Re}\chi_2 = 1.3 \cdot 10^{-11} \text{ CGSE units.}$$

In the same experiments, nonlinear absorption of light in the colloidal silver solution was measured. This allowed the value of the imaginary part of the sum of χ_1 and χ_2 to be determined

$$\mathrm{Im}(\chi_1 + \chi_2)\ [\mathrm{CGSE}] = 2\sqrt{2}\,\frac{\delta(e^{-2l\delta} - T)}{T(1 - e^{-2l\delta})} \times$$

$$\times \frac{cn_0\,\lambda\ [\mathrm{CGSE}]}{16\pi^3 \cdot 10^{13}\, I_0\ [\mathrm{MW/cm^2}]} \approx -1.1 \cdot 10^{-10}, \quad (12)$$

where T is the transmittance (for the intensity) with the allowance for both linear and nonlinear absorption; $\delta = 1.15$ cm^{-1} is the amplitude coefficient of linear absorption; $l = 3$ mm is the radiation path length in the nonlinear medium; I_0 is the peak intensity on the beam axis before entering the cell. In the experiment, the transmittance was $T \approx 0.65$ at $I_0 \approx 6$ MW/cm^2.

Now let us describe the experiments with the probe field.

Optical Kerr effect. To measure the value of the optical Kerr effect, we used the experimental setup shown schematically in Fig. 1. The polarization direction of the probe beam made a 45° angle with that of the strong beam. A phase element was set on the path of the probe beam after the cell for introducing the phase difference between its x- and y-components. Then the probe beam passed through an analyzer oriented as in the previous case (with the axis at an angle of 45° with respect to the x axis). The beams separated by the analyzer came to photodetectors, whose signals can be represented as

$$I_1 = \frac{1}{2}\,(|S_x|^2 + |S_y|^2 - 2|S_x|\,|S_y|\,\cos\Delta\varphi),$$

$$I_2 = \frac{1}{2}\,(|S_x|^2 + |S_y|^2 + 2|S_x|\,|S_y|\,\cos\Delta\varphi), \quad (13)$$

where $\Delta\varphi$ is the phase difference between the components x and y. The parameter $\Delta\varphi$ is the sum of the nonlinear phase shift $\Delta\varphi^{nl}$ incurred in the medium and the phase difference introduced by the phase element $\Delta\varphi_0$:

$$\Delta\varphi = \Delta\varphi_0 + \Delta\varphi^{nl}. \quad (14)$$

In the experiments, we measured the difference of signals, $I_2 - I_1$; at a small nonlinear phase shift, it can be written as

$$\Delta I \equiv I_2 - I_1 \approx 2|S_x|\,|S_y|(\cos\Delta\varphi_0 - \Delta\varphi^{nl}\sin\Delta\varphi_0). \quad (15)$$

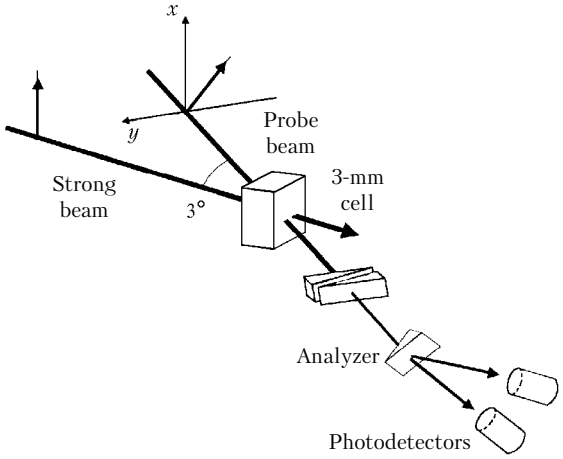

Fig. 1. Layout of the experimental setup for studying the optical Kerr effect.

The phase element introduces the shift $\Delta\varphi_0 = -\pi/2$, and the nonlinear shift is expressed in terms of the measured parameters (taking into account that $|S_x| = |S_y|$) as

$$\Delta\varphi^{nl} = \Delta L/2|S_x|^2. \quad (16)$$

The results of OKE measurements for our samples are shown in Fig. 2. The experimentally determined nonlinear phase shift between the x- and y-components of the probe beam is plotted as a function of the pump intensity.

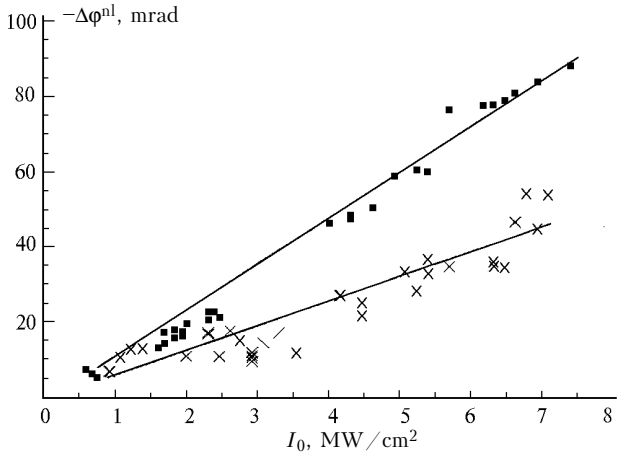

Fig. 2. Nonlinear phase shift between the x- and y-components of the probe field as a function of the intensity of the strong field: colloid 1 (closed squares) and colloid 2 (crosses).

Inverse Faraday effect. Unlike the experimental setup shown in Fig. 1, in the experimental setup for

studying IFE, a phase element was used in the path of the strong beam before the cell with the colloid. The phase element imparted the clockwise circular polarization to the strong beam. The measured parameter in the experiment was the angle of rotation of the probe beam polarization plane. This beam was directed to the analyzer, whose axes were oriented at the angle of 45° with respect to the axis x. The analyzer separated the probe field into two orthogonally polarized beams, which then came to the photodetectors. The signals from the photodetectors can be expressed in terms of the angle α between the axis x and the polarization plane of the probe field:

$$I_1 = |S_x|^2 \cos^2(45° - \alpha), \quad I_2 = |S_x|^2 \sin^2(45° - \alpha). \quad (17)$$

At a small α, the approximate equality

$$\alpha \approx \frac{I_1 - I_2}{2|S_x|^2} = \frac{\Delta I}{2|S_x|^2} \quad (18)$$

is valid.

Figure 3 shows the dependence of the rotation angle of the polarization plane of the probe beam in the IFE experiment on the intensity of strong beam for the two colloidal solutions with different degrees of aggregation. The angle α was determined by Eq. (18).

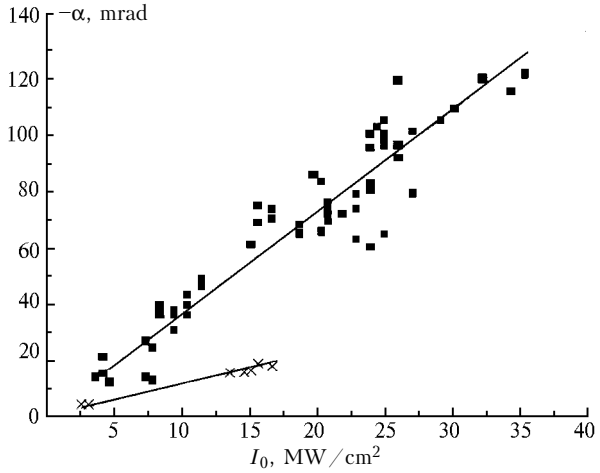

Fig. 3. Rotation angle of the polarization plane of the probe field as a function of the intensity of the strong field with circular polarization: colloid 1 (closed squares) and colloid 2 (crosses).

It is worth noting that these experiments did not reveal saturation of neither IFE nor OKE with the increase of the incident radiation intensity up to 35 MW/cm^2.

Let us now determine the constants of cubic nonlinearity from the experimental data. From the IFE measurements we can find the difference $\chi_1 - 2\chi_2$:

$$\mathrm{Re}\,(\chi_1 - 2\chi_2)\ [\mathrm{CGSE}] = 2\sqrt{2}\,\frac{\lambda\alpha}{l}\,\frac{n_0^2\, c\ [\mathrm{CGSE}]}{4\pi^3 \cdot 10^{13}\, I_{\mathrm{eff}}\ [\mathrm{MW/cm^2}]}, \quad (19)$$

where the effective intensity $I_{\mathrm{eff}} = \left(\int_0^l I(z)\mathrm{d}z\right) \Big/ l$ is introduced to take into account extinction of the strong field due to linear absorption in the medium. Absorption in the high-aggregated colloid with the cell thickness $l = 3$ mm was 50%. This value corresponds to $I_{\mathrm{eff}} \approx 0.72 I_0$, where I_0 is the pulse peak intensity on the beam axis before entering the cell. Substituting the values from Fig. 3, we have $\mathrm{Re}(\chi_1 - 2\chi_2) = -(1.14 \pm 0.06) \cdot 10^{-10}$ CGSE units for the colloid 1, $\mathrm{Re}(\chi_1 - 2\chi_2) = -(3.6 \pm 0.25) \cdot 10^{-11}$ CGSE units for the colloid 2.

The value of birefringence due to OKE is proportional to the sum of nonlinear coefficients χ_1 and $2\chi_2$. Approximating the data from Fig. 2 by a linear function, we find $\mathrm{Re}(\chi_1 + 2\chi_2) = -(1.9 \pm 0.24) \cdot 10^{-10}$ CGSE units for the colloid 1 and $\mathrm{Re}(\chi_1 + 2\chi_2) = -(9.0 \pm 3.6) \cdot 10^{-11}$ CGSE units for the colloid 2.

Combining the results of IFE and OKE measurements, we can find χ_1:

$\mathrm{Re}\chi_1 = -(1.5 \pm 0.15) \cdot 10^{-10}$ CGSE units for the colloid 1

$\mathrm{Re}\chi_1 = -(6.0 \pm 1.8) \cdot 10^{-11}$ CGSE units for the colloid 2.

It should be noted that the value $\chi_2 = -(1.9 \pm 0.75) \cdot 10^{-11}$ CGSE units, which can be determined from the IFE and OKE measurements, significantly (even in the sign) differs from the value determined from measurements of the self-induced rotation of the polarization ellipse. No satisfactory explanation of this discrepancy has been found until so far.

The polarization measurements of $\mathrm{Re}(\chi_1 + \chi_2)$ and measured $\mathrm{Im}(\chi_1 + \chi_2)$ [recall that $\chi_{1111} = (\chi_1 + \chi_2)/3$] give the value $|\chi_{1111}| \approx 6.7 \cdot 10^{-11}$ CGSE. This value is close to the susceptibility of the aggregated aqueous colloid ($|\chi_{1111}| \sim 10^{-10}$ CGSE) measured from the efficiency of degenerated four-photon scattering (DFS) (Ref. 4) at the wavelength of 532 nm and far exceeds the nonlinear susceptibility of monomers $|\chi_{1111}| \sim 10^{-13}$ CGSE (Ref. 22). According to our measurements of OKE and IFE, the nonlinear susceptibility increases most markedly at the initial stage of aggregation, at which monomers form small aggregates consisting of two or three nanoparticles. (Note that this result agrees with the data from Ref. 4 obtained for the aqueous borane colloid by the DFS method.) The further increase of clusters up to 100–1000 particles causes weaker growth of $\chi^{(3)}$. This means that the key point in achieving an enhancement of nonlinear responses is creation of conditions for the collective resonance at the frequency of incident radiation. In practice, this can be done already in the case of two sufficiently closely separated monomers thanks to interactions among the induced dipoles (or multipoles). Actually, the increase of the local field

compared to the incident one for resonance modes in the binary approximation gives $E_{i\,\mathrm{res}}/E_0 \sim \varepsilon_1^2/3\varepsilon_0\,\varepsilon_2 = 18$ for $\lambda = 532$ nm, where $\varepsilon = \varepsilon_1 + i\varepsilon_2$ and ε_0 are the dielectric constants of a metal particle and the environment. This value is comparable with the numerically determined value of the enhancement factor for large aggregates.[12]

Conclusion

In this paper, we have studied the polarization effects in the aggregated colloidal silver solution due to cubic nonlinearity of the optical response with the allowance made for the spatial dispersion. The inverse Faraday effect, optical Kerr effect, and self-induced rotation of the polarization ellipse in silver nanocomposites were observed for the first time. The constant of nonlinear optical activity has been measured under same conditions.

The measurements of the components of the tensor $\hat{\chi}^{(3)}$ of local nonlinear susceptibility have shown that the nonlinear constants for the Ag(PVP) colloid did not decrease at least at the intensity ~ 35 MW/cm^2. We can likely say that no marked modification of the local configuration of monomers occurs in the range of intensities we had in the studies of this colloid. In other words, those groups of several monomers, for which the condition of the collective resonance is fulfilled, are mostly unchanged, and the large value of the nonlinear response keeps unchanged for this reason. At the same time, a decrease in the nonlocal nonlinearity at the intensity higher than some value is indicative of the threshold change of the aggregate structure with the dimensions close to the wavelength.

The polarization measurements have allowed us to estimate the ratio of the independent constants of local nonlinearity. The obtained ratio $\mathrm{Re}\chi_2/\mathrm{Re}\chi_1 \approx -0.09$ differs significantly from the typical values ~ 0.5 for solid-state media,[23] which are characteristic of nonresonance electronic mechanism of nonlinearity. This fact can be considered as an argument in favor of a significant role of the inertial contributions to the mechanism of nonlinearity of aggregated silver colloids at nanosecond pulses.

Acknowledgments

The work was partially supported by the Russian Foundation for Basic Research Grants No. 99-02-16670 and No. 01-02-06047, as well as by the US Civilian Research & Development Foundation (CRDF), Grant RE1-2229.

References

1. B.M. Smirnov, *Physics of Fractal Clusters* (Nauka, Moscow, 1991), 133 pp.
2. R.K. Chang and T.E. Furtak, eds., *Surface-Enhanced Raman Scattering* (Plenum Press, New York–London, 1982).
3. A.V. Butenko, V.M. Shalaev, and M.I. Shtokman, Zh. Eksp. Teor. Fiz. **94**, No. 1, 107–124 (1988).
4. S.G. Rautian, V.P. Safonov, P.A. Chubakov, V.M. Shalaev, and M.I. Shtokman, Pis'ma Zh. Eksp. Teor. Fiz. **47**, No. 4, 200–203 (1988).
5. I.A. Akimov, A.V. Baranov, V.M. Dubkov, V.I. Petrov, and E.A. Sulabe, Opt. Spektrosk. **63**, No. 6, 1276–1279 (1987).
6. Yu.E. Danilova, V.P. Drachev, S.V. Perminov, and V.P. Safonov, Izv. Ros. Akad. Nauk, Ser. Fiz. **60**, 18–22 (1996).
7. N.N. Lepeshkin, W. Kim, V.P. Safonov, J.G. Zhu, R.L. Armstrong, C.W. White, R.A. Zuhr, and V.M. Shalaev, J. Nonlinear Optical Physics and Materials **8**, No. 2, 191–210 (1999).
8. R.A. Ganeev, A.I. Rasnyanskii, and T. Usmanov, Kvant. Elektron. **31**, 185–186 (2001).
9. W. Kim, V.P. Safonov, V.M. Shalaev, and R.L. Armstrong, Phys. Rev. Lett. **82**, No. 24, 4811–4814 (1999).
10. Yu.E. Geints, A.A. Zemlyanov, V.E. Zuev, A.M. Kabanov, and V.A. Pogodaev, *Nonlinear Optics of Atmospheric Aerosol* (SB RAS Publishing House, Novosibirsk, 1999), 260 pp.
11. V.A. Markel', L.S. Muratov, and M.I. Shtokman, Zh. Eksp. Teor. Fiz. **98**, No. 3, 819–837 (1990).
12. V.M. Shalaev, *Nonlinear Optics of Random Media: Fractal Composites and Metal-Dielectric Films* (Springer-Verlag, Berlin, 1999), 158 pp.
13. M.I. Stockman, Phys. Rev. E **56**, No. 6, 6494–6507 (1997).
14. V.P. Safonov, V.M. Shalaev, V.A. Markel, Yu.E. Danilova, N.N. Lepeshkin, W. Kim, S.G. Rautian, and R.A. Armstrong, Phys. Rev. Lett. **80**, No. 5, 1102–1105 (1998).
15. Yu.E. Danilova, V.A. Markel', and V.P. Safonov, Atmos. Oceanic Opt. **6**, No. 11, 821–826 (1993).
16. V.P. Drachev, S.V. Perminov, S.G. Rautian, V.P. Safonov, Pis'ma Zh. Eksp. Teor. Fiz. **68**, No. 8, 618–622 (1998).
17. P. Maker, R. Terhune, and C. Savage, Phys. Rev. Lett. **12**, No. 11, 507–509 (1964).
18. V.M. Arutyunyan, T.A. Papazyan, G.G. Adonts, A.V. Karmenyan, S.P. Ishkhanyan, and L. Khol'ts, Zh. Eksp. Teor. Fiz. **68**, No. 1, 44–50 (1975).
19. A.M. Bonch-Bruevich, N.N. Kostin, and V.A. Khodovoi, Pis'ma Zh. Eksp. Teor. Fiz. **3**, No. 11, 425–429 (1966).
20. S.A. Akhmanov, G.A. Lyakhov, V.A. Makarov, and V.I. Zharikov, Optica Acta **29**, No. 10, 1359–1369 (1982).
21. H. Hirai, J. Mastrom. Sci. Chem. **A13**, 633–649 (1979).
22. D. Ricard, P. Roussignol, and C. Flytzanis, Opt. Lett. **10**, No. 10, 511–513 (1985).
23. A.N. Azarenkov, G.V. Al'tshuler, N.R. Belashenkov, and S.A. Kozlov, Kvant. Elektron. **20**, No. 8, 733–757 (1993).